

# Secure communication using mesoscopic coherent states

Geraldo A. Barbosa\*, Eric Corndorf, Prem Kumar, and Horace P. Yuen

*Center for Photonic Communication and Computing,*

*Department of Electrical and Computer Engineering, Northwestern University, Evanston, IL 60208*

(Dated: December 3, 2002)

We demonstrate theoretically and experimentally that secure communication using intermediate-energy (mesoscopic) coherent states is possible. The quantum noise inherent to coherent states can be used to hide a bit with the eavesdropper's error probability approaching the pure-guessing value  $P_e^E = 1/2$  under individual attacks. This encryption scheme can be optically amplified. New avenues are open to secure communications at high speeds in fiber-optic or free-space channels.

For the encryption of data with perfect secrecy [1] that cannot be broken with any advance in technology, one may in principle employ one-time pad with secret key obtained by the BB84 [2] quantum cryptographic technique for key expansion. Such an approach is, however, slow and inefficient because the key length needs to be as long as the data, and it also requires a nearly ideal quantum communication line that is especially difficult if not impossible to obtain in commercial systems [3]. On the other hand, for both military and commercial applications, there are great demands for secret communications that are fast and secure but not necessarily perfectly secure. (There are many practical issues, human as well machine based, that would make theoretical perfect security in specific models not so important in real life [4]). In the following, a new scheme based on ideas similar to those of Ref. [5] is described for secure data encryption that can be operated at optical speeds with conventional optical technology, and a prototype experimental implementation is presented.

The following line of reasoning describes the ideas [6] that led to the development of our present kind of quantum cryptographic schemes. One crucial element for obtaining security in BB84 involves the detection of small intrusion on weak signals, which is difficult to achieve in a network environment. This problem would be alleviated if quantum signal sets of higher intensity are selected for different bit values by a secret key shared between the sender (Alice) and the receiver (Bob). It is important to remember that some shared secret key is needed in BB84 for message authentication during protocol execution. The resulting scheme is acceptable as key expansion if the new key is secure even if the shared secret key is known to the attacker after the user communications are completed. When a secret key is used to identify the signal set, it would be a secret CDMA (Code Division Multiple Access) scheme classically, which does not allow key expansion because the user and the attacker have the same observation. We would discuss elsewhere how a corresponding KCQ (Keyed CDMA in Quantum Noise) scheme can be used to obtain key expansion in the quantum case. In this paper, we are concerned with the use of KCQ for data encryption.

There are two basic problems with classical encryp-

tion that does not employ the inefficient one-time pads. One is that the total data uncertainty  $H(\mathbf{X})$  given observation  $\mathbf{Y}$  is bounded above by the key uncertainty,  $H(\mathbf{X}) \leq H(\mathbf{K})$  [1]. The other is that the key  $\mathbf{K}$  may be found by a *known-plaintext attack* when the eavesdropper (Eve) knows the output-input pairs  $(\mathbf{Y}, \mathbf{X})$  for some data length. In our scheme,  $H(\mathbf{X})$  is not bounded by  $H(\mathbf{K})$  because Eve cannot have the observation  $\mathbf{Y}$  that Bob obtained via the *optimal quantum* measurement utilizing the key  $\mathbf{K}$ . To extract information from even a full copy of the quantum signal without knowing  $\mathbf{K}$ , Eve has to make a sub-optimal measurement that would yield information on all possible signal sets for the purpose of either estimating  $\mathbf{X}$  or finding  $\mathbf{K}$  from a known-plaintext attack. As a result, Bob has a better channel/observation than Eve so that, in contrast to classical cryptography, one can *prove* the security of our scheme against ciphertext-only attacks, although only individual attacks are described in this paper. Also, one can show that even an exponentially powerful search with known-plaintext attacks cannot succeed here because Eve does not have  $\mathbf{Y}$  as above. Practically, our scheme can run at high speeds because there is no need for a long key  $\mathbf{K}$ .

Consider the following scheme in which each data bit is encoded into a coherent state of an infinite-dimensional space, referred to as a "qumode". As in [5], there are  $M$  possible states

$$|\alpha_0(\cos \theta_l + i \sin \theta_l)\rangle, \theta_l = 2\pi l/M \quad (1)$$

for a real  $\alpha_0$  and  $l \in \{0, \dots, M-1\}$ , forming  $M/2$  pairs  $\{l, l + M/2\}$ . A *seed key*  $\mathbf{K}$  is used to drive an encryption mechanism whose output is a much longer *running key*  $\mathbf{K}'$  that is used to determine, for each qumode carrying bit  $b$  ( $= 0, 1$ ), which pair of signals (signal set) is to be used. Each pair may be macroscopically distinguishable since the inner product of any two basis states is  $\exp(-2|\alpha_0|^2)$ . For large  $M$ , a lower bound on the obtained mean-square error  $(\delta\theta)^2$  [7] that goes as  $1/|\alpha_0|^2$  shows that asymptotically when  $M \gg |\alpha_0|$  the attacker's error probability  $P_e^E$  tends to  $1/2$ , the guessing level, in an individual attack on the data bit  $b$ . That this result holds in the limit  $M \rightarrow \infty$  for fixed  $|\alpha_0|$  is intuitively obvious. A two-mode coherent-state realization similar to Eq. (1), with  $|\alpha_0 \cos \theta_l\rangle|\alpha_0 \sin \theta_l\rangle$ , can also be used

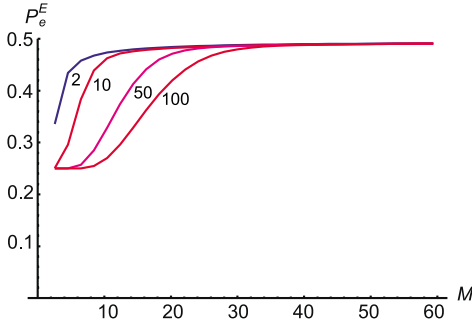


FIG. 1:  $P_e^E$  as a function of  $M$  for  $|\alpha|^2 = 2, 10, 50, 100$ .

and the modes can be interpreted as ones of polarization, time, frequency, or whatever.

Numerical calculation of the optimal POVM for individual attack on bit discrimination for the  $M$ -ry case has shown [8] that the minimum probability of error  $P_e^E$  for an eavesdropper can be made arbitrarily close to  $1/2$  for a given coherent-state amplitude  $\alpha$ . The value  $P_e^E \rightarrow 1/2$  for a fixed average number of photons  $|\alpha|^2$  is achieved by increasing the number of levels  $M$ . As shown in Figure 1,  $P_e^E$  goes very fast to the asymptotic pure-guessing limit of  $1/2$  as  $M$  increases. The above POVM calculation demonstrates that in this scheme an eavesdropper cannot obtain the bits sent regardless of the precision of her devices. The optimal POVM gives the maximum amount of information she could obtain from the sequence of physical signals sent without knowing the key. This uncertainty is due to the quantum noise of light and cannot be overcome with one's precision capabilities. Bob, on the other hand, by knowing the key can extract information with greater precision. His decision has to be made only between two nearly orthogonal states in the same basis defined by a given  $\mathbf{K}'$ . His probability of error is [9]  $P_e^B = \frac{1}{2} \left( 1 - \sqrt{1 - e^{-2|\alpha|^2}} \right)$ . For large values of  $|\alpha|$  the minimum probability of error  $P_e^B$  is negligible, which makes possible an excellent signal recovery by the legitimate receiver. The case of collective attacks is more complicated and cannot be discussed here, in large part because there is no meaningful approach for evaluating the optimal bit error, even in the classical case. However, the entropy bound (Holevo's theorem) could be used to show the ideal nature of this scheme for the criterion of data entropy.

The attacker can also try to find the key  $\mathbf{K}$  based on her copy of the quantum signals, with or without some known-plaintext (data) corresponding to the signals. Even in a known-plaintext attack, the signal quantum fluctuation would yield, from the number of possibilities in each qumode, an exponential number of possible  $\mathbf{K}'$  in a sequence of data bits. To identify  $\mathbf{K}$  from such noisy observations of possible  $\mathbf{K}'$  would involve an exponential search, which can always be launched against

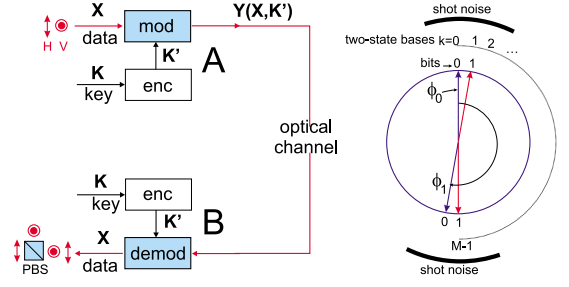


FIG. 2: *Left side:* Basic ciphering scheme with qumodes of polarization. *Right side:* Two neighboring bases in an  $M$ -ry manifold on a great circle of Poincaré's sphere. Bits 0 and 1 are antipodals for each basis. Closest states (similar polarization ellipses) represent *opposite* bit values.

a key in known-plaintext attacks but which is currently believed to be proven impossible computationally even with a quantum computer. More significantly, Eve cannot succeed because, not knowing  $\mathbf{K}$ , she does not have a good observation  $\mathbf{Y}$  similar to Bob's to begin with. Note that the attacker has a much more difficult job of estimating the signal pair from  $M/2$  possible ones, than the user who tries to discriminate 2 possible known states. A detailed quantitative treatment would be given elsewhere. It is important to note that, in the case of classical cryptography, if the running key  $\mathbf{K}'$  is used directly as one-time pad on the data, the result is well known [10] to be insecure against known-plaintext attacks. In our case, this attack is thwarted by quantum effects as explained above.

Consider an implementation of the above scheme as depicted in Fig. 2. This particular type of KCQ scheme will be referred to as  $\alpha\eta$  (for coherent states and efficiency). In the encryption scheme for this new protocol, sketched on the left side in Fig. 2, Alice uses an explicit short secret key  $\mathbf{K}$ , extended to a longer key  $\mathbf{K}'$  by another encryption mechanism such as a stream cipher, to modulate the parameters of a multimode coherent state. For the free-space implementation to be presented, the qumodes are the two orthogonal modes of polarization. In this case, Alice uses the running key  $\mathbf{K}'$  to specify a polarization basis from a set of  $M/2$  uniformly spaced two-mode bases spanning a great circle on the Poincaré sphere, as shown on the right in Fig. 2. Each basis consists of a polarization state and its antipodal state at an angle  $\pi$  from it, representing the 0 and 1 bit value for that basis.

The message  $\mathbf{X}$  is encoded as  $\mathbf{Y}(\mathbf{X}, \mathbf{K}')$ . This mapping of the stream of bits onto points on the surface of the Poincaré sphere is the information to be shared by Alice (A) and Bob (B). Because of his knowledge of  $\mathbf{K}'$ , Bob is able to make a precise demodulation operation, producing the plaintext  $\mathbf{X}$ . He uses  $\mathbf{K}'$  to apply the requisite polarization transformation to the received sequence of polarization states to return them to the linearly orthog-

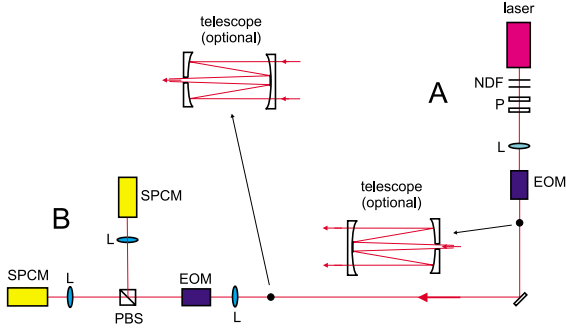


FIG. 3: Schematic of the experimental setup. SPCM, single photon counting module; PBS, polarization beamsplitter; L, lens; P, polarizer; NDF, neutral density filter. Two (optional) telescopes are shown for field work.

onally polarized condition, representing the two original bits of the message  $\mathbf{X}$ . Bob's demodulation is the inverse mapping transformation that was utilized by Alice.

Figure 3 shows a table-top experimental setup we have implemented as a proof-of-principle demonstration of this scheme. The modulation systems utilized both at the transmitter and receiver ends are electro-optic modulators (EOMs) (New Focus, model 4104), the laser (Toshiba, model TOLD9225M) operates at 670nm, and the detectors are single photon counting modules (Perkin-Elmer, model SPCM-AQR-16) with interference filters of 10nm bandwidth in front. A polarization beam splitter (PBS) is used at the receiver to discriminate between the orthogonal linear polarization states. Lenses (L) are used to optimize the beam Rayleigh range within the EOMs. A personal computer containing an interface card (National Instruments, model PCI-6111E) is used to control the EOM's (digital-to-analog operation). The same card is also used for counting the output pulses from the detectors. In this configuration, a horizontally (H) or vertically (V) polarized light pulse representing bit 0 or 1 is generated and transformed into an elliptically polarized light state by application of the voltage  $V_k$  ( $k \in \mathbf{K}'$ ). This voltage introduces a phase difference  $\Delta\phi_k$  between the physical axes of the EOM, where  $\Delta\phi_k = \frac{\pi}{2} \frac{V_k}{V_\pi} + \phi_0$ , and  $V_\pi$  and  $\phi_0$  are specific to each modulator. This system operates, with bulk optics, at 200kHz rate for demonstration purposes and faster fiber based systems ( $\sim 1\text{GHz}$ ) are being implemented for free space as well as fiber channels.

Figure 4 shows a sequence of bits as received by Bob. The clear separation of the 0 and 1 histograms allow him to make bit decisions with no error. The same sequence of bits as seen by Eve are shown in Fig. 5, giving her a very high probability of error ( $P_e^E \sim 1/2$ ) in bit decisions because of her lacking the key.

As an illustration of how the quantum noise of light can be utilized by the legitimate receiver on his behalf, in Fig. 6 we show the uncertainty in the polarization an-

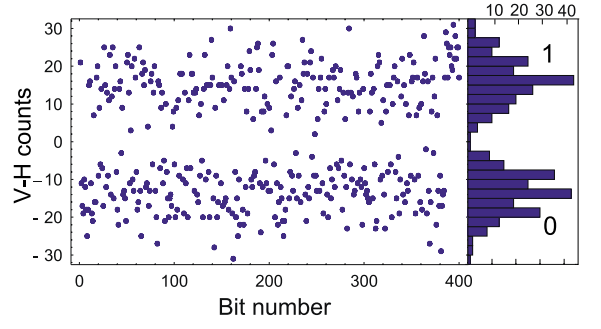


FIG. 4: Difference of V and H counts (V-H) from Bob's receiver operating at 200kHz, with the average number of received photons  $\langle n \rangle = |\alpha|^2 = 27$  and  $M = 50$ . The right inset shows the corresponding histogram indicating clear separation between the 0 and 1 bit values.

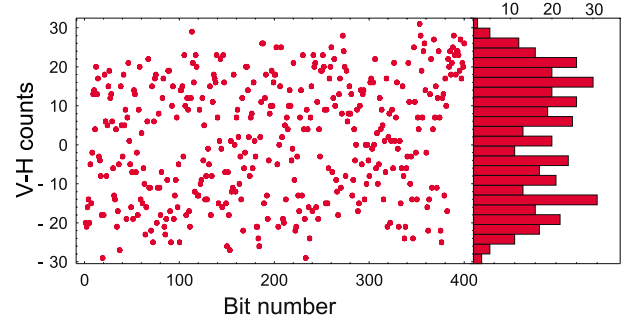


FIG. 5: V-H counts from Eve's receiver in an opaque attack in which she takes all the power from the channel that would have gone to Bob. All operating parameters are the same as in Fig. 4, except for Eve lacking the key  $\mathbf{K}'$ . The corresponding histogram on the right shows that distinct bits are not distinguishable by her.

gle produced by a two-mode measurement for an average total photon number  $\langle n \rangle \simeq 38$ . Regions of low-variance values are seen around 0 and  $\pi/2$  settings of the input polarization state [cf. Fig. 6(c)]. Such determination of the polarization angle with angle-dependent uncertainty shows that a higher degree of precision in angle determination can be achieved by an observer with a prior information on how to set the measuring apparatus than another who does not have this knowledge. From Fig. 6(c) one can observe that for PBS-axis orientations close to the incoming field polarization direction the uncertainty in determination of the angle is small. The polarization angle is obtained by averaging  $\arctan \sqrt{n_V/n_H}$  over the occurrence of  $n_H$  and  $n_V$ , the photon numbers reaching the detectors [cf. Fig. 6(b)]. The approximation that  $\theta$  can be obtained through  $\arctan \sqrt{n_V/n_H}$  is adequate for mesoscopic signals but becomes inadequate as  $\langle n \rangle \rightarrow 0$  (quantum phase domain). Setting PBS without knowledge of this preferred orientation leads, in average, to a larger error in determination of the polarization angle. On the other hand, an observer setting his analyzer system close to the field polarization direction (0 or  $\pi/2$ ) is

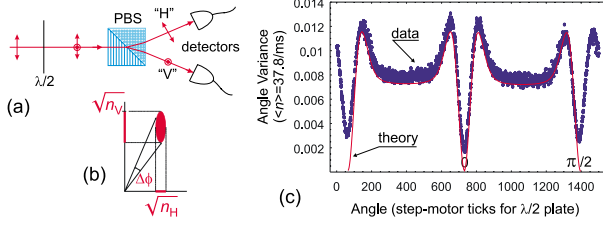


FIG. 6: (a) Measurement of the polarization angle through two-mode direct detection with use of a PBS. A  $\lambda/2$  waveplate is rotated to produce different polarization angles  $\phi$ . (b) Uncertainties in  $\phi$ ,  $\Delta\phi$ , arise owing to photon-number fluctuations around  $\langle n_H \rangle$  and  $\langle n_V \rangle$ , where  $n_H$  and  $n_V$  are the photon numbers sampled by the two detectors ( $\langle n_H n_V \rangle = \langle n_H \rangle \langle n_V \rangle$ ). (c) Variance in the angle  $\phi$  obtained via the two-mode measurement versus the angle set by the  $\lambda/2$  plate. Solid line is the theoretical prediction, not a fit, *without* considering the detector noises (mainly “dark” and Johnson noises), which will set the ultimate precision limit in these measurements.

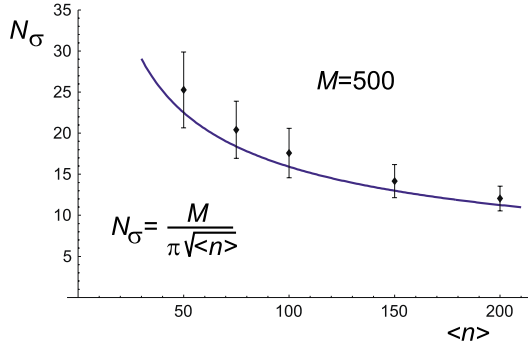


FIG. 7: Number of bases  $N_\sigma$  covered by the quantum noise as a function of the number of photons  $\langle n \rangle = |\alpha|^2$ . For a given  $\langle n \rangle$ , Alice repeatedly sets every basis, separated by  $\pi/M$  ( $M = 500$ ), one by one, by applying a voltage to the EOM. By measuring  $n_H$  and  $n_V$ , Eve performs an angle reconstruction in an attempt to identify the basis used. Eve’s standard deviation around the basis sent by Alice gives  $N_\sigma$ . Line is the theory.

only limited by the optical precision of the analyzer used (which can be made arbitrarily small), and the noise in the detectors.

The cryptography system should be designed so that the uncertainties caused by the quantum noise of light in the measurement of the polarization angles is large. It can be shown that the number of bases  $N_\sigma$  covered by the quantum noise is  $N_\sigma = M/(\pi|\alpha|)$ . Fig. 7 shows experimental results that confirm this dependence.

The effect of noise on signal recovery by an eavesdropper in an opaque attack can be simulated by sending repeatedly the same bit, but varying  $\mathbf{K}'$ , from A to B when B (playing Eve) does not apply the key to demodulate the signals. In the following sequence  $S$ ,

the first number in a brace is the basis set by Alice (selected from  $M = 200$  possible positions with  $N_\sigma \simeq 6$ , and correctly recovered by Bob with the use of the key) while the second number is the basis extracted by Eve through a *single* measurement of  $n_H$  and  $n_V$ .  $S = \{110, 117\}, \{84, 78\}, \{108, 99\}, \{90, 91\}, \{100, 107\}, \{102, 97\}, \{84, 84\}, \{110, 105\}, \{110, 111\}, \{114, 105\}, \{82, 86\}, \{100, 95\}, \{92, 72\}, \{108, 108\}, \{102, 90\}, \{108, 97\}, \{96, 93\}, \{110, 103\}, \{112, 121\}, \{86, 86\}, \{102, 100\}, \{88, 91\}, \{102, 94\}, \{106, 98\}, \{118, 135\}$ . Clearly, Eve makes a large number of errors, since neighboring bases are used to encode opposite bit values.

In conclusion, we have demonstrated that under individual attacks, Yuen’s encryption protocol gives unconditional security with an adequate number of bases  $M$ . Key expansion is also possible under this scheme, due to the better observation available to Bob with knowledge of the key. Significantly, the encryption system allows for signal *amplification* as long as the security is guaranteed at the source for the following reason. While Eve has to resolve  $M$  levels to tell the bit or  $\mathbf{K}'$  without knowing the key, Bob has to resolve only two levels with the key. Thus, amplifier noise would hinder Eve’s attack while it will not disrupt Bob’s decryption. Furthermore, there is no need to decrypt/re-encrypt at the nodes of a properly designed communication line with a moderate number of amplifiers.

**Acknowledgements** – This work is supported by the DARPA grant F30602-01-2-0528. We thank Adam Rybaltovski for some help in the early stages of this work and Paul Voss for advice on data acquisition programming. \*E-mail: barbosa@northwestern.edu.

- [1] C. E. Shannon, Bell Syst. Tech. J. **28**, pp. 656-715, 1949.
- [2] C. H. Bennett and G. Brassard, in Proc. of the IEEE Int. Conf. on Computers, Systems and Signal Processing, Bangalore, India, pp. 175-179, 1984.
- [3] N. Gisin, G. Ribordy, W. Tittel, and H. Zbinden, Rev. Mod. Phys. **74**, pp. 145-195 (2002).
- [4] B. Schneier, “Secrets and Lies”, Wiley, New York, 2000.
- [5] H. P. Yuen, in Quantum Communications, Computations, and Measurements III, Plenum Press, 2001.
- [6] H. P. Yuen, to be published.
- [7] H. P. Yuen, in Quantum Squeezing, Springer-Verlag, to be published; also in quant-ph0109054.
- [8] G. A. Barbosa, E. Corndorf, P. Kumar, H. P. Yuen, G. Mauro D’Ariano, M. G. A. Paris, and P. Perinotti, Int. Conf. on Quantum Communication, Measurement and Computing, July 2002 (Rinton Press).
- [9] C. W. Helstrom, *Quantum Detection and Estimation Theory*, (Academic Press, 1976).
- [10] A. J. Menezes, P. C. van Oorschot, and S. A. Vanstone, “Handbook of Applied Cryptography”, CRC Press, New York, ch. 6, 1997.